

Adsorption of cesium on cement mortar from aqueous solutions

Konstantin Volchek^{a,*}, Muhammed Yusuf Miah^{a,b}, Wenxing Kuang^a, Zack DeMaleki^a, F. Handan Tezel^c

^a Emergencies Science and Technology Section, Environment Canada, 335 River Road, Ottawa, Ontario, Canada K1A 0H3

^b Department of Applied Chemistry and Chemical Technology, Noakhali Science and Technology University, Bangladesh

^c Department of Chemical and Biological Engineering, University of Ottawa, 161 Louis-Pasteur, Ottawa, Ontario, Canada K1N 6N5

ARTICLE INFO

Article history:

Received 12 March 2011

Received in revised form 27 July 2011

Accepted 28 July 2011

Available online 7 August 2011

Keywords:

Cesium

Cement mortar

Concrete

Adsorption

Kinetic

Equilibrium

ABSTRACT

The adsorption of cesium on cement mortar from aqueous solutions was studied in series of bench-scale tests. The effects of cesium concentration, temperature and contact time on process kinetics and equilibrium were evaluated. Experiments were carried out in a range of initial cesium concentrations from 0.0103 to 10.88 mg L⁻¹ and temperatures from 278 to 313 K using coupons of cement mortar immersed in the solutions. Non-radioactive cesium chloride was used as a surrogate of the radioactive ¹³⁷Cs. Solution samples were taken after set periods of time and analyzed by inductively coupled plasma mass spectroscopy.

Depending on the initial cesium concentration, its equilibrium concentration in solution ranged from 0.0069 to 8.837 mg L⁻¹ while the respective surface concentration on coupons varied from 0.0395 to 22.34 μg cm⁻². Equilibrium test results correlated well with the Freundlich isotherm model for the entire test duration. Test results revealed that an increase in temperature resulted in an increase in adsorption rate and a decrease in equilibrium cesium surface concentration. Among several kinetic models considered, the pseudo-second order reaction model was found to be the best to describe the kinetic test results in the studied range of concentrations. The adsorption activation energy determined from Arrhenius equation was found to be approximately 55.9 kJ mol⁻¹ suggesting that chemisorption was the prevalent mechanism of interaction between cesium ions and cement mortar.

Crown Copyright © 2011 Published by Elsevier B.V. All rights reserved.

1. Introduction

Radioactive cesium (¹³⁷Cs) is a common radionuclide that has a range of applications such as cancer therapy, radiation detection, mineral processing, and construction industry. Cesium is also one of the main products of nuclear fission and is therefore present in spent nuclear fuel [1,2]. Release of the radioactive cesium into environment can create serious environmental problems as well as human health hazard. Well known examples of such releases include the accident at the Chernobyl Nuclear Power Plant [3,4], incidents in Goiânia, Brazil [5] and in Los Barrios, Spain [6]. In these cases, the release of cesium resulted in an environment contamination whose mitigation required significant efforts. In addition to accidental releases, radioactive cesium can enter the environment as a result of sabotage of terrorism, e.g., using a radiological dispersal device, or “dirty bomb” [7].

Given the abundance of sources of radioactive cesium and its damaging effects, there has been extensive research on the adsorption of cesium on various materials [7–14]. For example,

the adsorption of cesium on ceiling tiles was investigated in our previous study [7]. Among various materials, cement-based construction materials such as concrete and mortar are of a particular interest in case of cesium release in an urban area, for two main reasons. First, cement is the main component of construction materials used in residential, commercial and industrial buildings. Cesium can therefore precipitate on cement mortar or concrete from the air as a result on an industrial accident. In addition to building construction materials, there are also concrete and cement-lined steel pipes widely used in drinking water distribution systems and in wastewater collectors. In this case, cesium can interact with cement mortar or concrete if cesium is present in radioactively contaminated water. Second, cesium can strongly bind to cementitious matrices which makes radiological decontamination difficult if not impossible [15]. The strong adsorption was explained by strong bonding that occurs between cesium and the silicates on the surface of concrete [16]. Cement contains oxides of calcium, aluminum, and silicon, commonly called as calcium–aluminum–silicate [17]. Microporosity of cementitious matrices also plays role in a high affinity towards cesium ions. A strong adsorption hinders the removal of cesium from contaminated concrete as reported by Real et al. [15].

It was reported that if cesium remains on concrete in a dry form it can be easily removed from the contaminated surface [4]. The

* Corresponding author. Tel.: +1 613 990 4073; fax: +1 613 991 9485.

E-mail address: konstantin.volchek@ec.gc.ca (K. Volchek).

Nomenclature

A	Arrhenius constant
b	Langmuir constant ($\text{mg}^{-1} \text{L}$)
C_0	initial cesium concentration in solution (mg L^{-1})
C_t	cesium concentration in the liquid phase at time, t (mg L^{-1})
C_e	cesium concentration in solution at equilibrium (mg L^{-1})
dq/dt	rate of adsorption ($\text{mg cm}^{-2} \text{h}^{-1}$)
E_a	activation energy (kJ mol^{-1})
k_1	first order rate constant for adsorption (h^{-1})
k_2	Pseudo second order rate constant for adsorption ($\text{cm}^2 \mu\text{g}^{-1} \text{h}^{-1}$)
K_F	Freundlich constant ($\mu\text{g}^{1-1/n} \text{mL}^{1/n} \text{cm}^{-2}$)
k_p	intra-particle diffusion constant ($\mu\text{g cm}^{-2} \text{h}^{-1/2}$)
m	coupon mass (g)
m_{av}	average coupon mass (g)
n	dimensionless Freundlich parameter ($n > 1$)
q_0	initial cesium surface concentration ($\mu\text{g cm}^{-2}$)
q_e	cesium surface concentration at equilibrium ($\mu\text{g cm}^{-2}$)
q_m	maximum saturation capacity ($\mu\text{g cm}^{-2}$)
q_t	cesium surface concentration at a given time ($\mu\text{g cm}^{-2}$)
R	universal gas constant ($8.314 \text{J K}^{-1} \text{mol}^{-1}$)
S	external surface area of the coupons (cm^2)
S_{av}	average external surface area of the coupons (cm^2)
T	temperature (K)
t	contact time (h)

presence of water, on the other hand, greatly enhances cesium binding to cementitious materials and makes its removal difficult. Water will most likely be present when cesium is released in the environment. For example, even if the original source of cesium is in a form of dry powder of cesium chloride, which is a common chemical form of radioactive cesium, the hygroscopic powder will quickly attract water if there is moisture in the air. In case of rain, cesium will dissolve in a large volume of water.

The objective of this study was to investigate the adsorption of cesium from aqueous solutions on cement mortar to mimic wet conditions and to address the case of a strong binding. Specific focus was on adsorption equilibrium and kinetics. This was to establish (a) what levels of contamination of cement mortar will be achieved for given cesium concentrations in solution and (b) how soon these levels will be achieved. Physicochemical modeling was used to interpret the experimental results. The goal was also to identify the nature of adsorption (i.e., physical or chemical) by estimating the value of adsorption activation energy.

Results of this study can likely be used to describe the adsorption of cesium on concrete. The difference between cement mortar and concrete is that the latter also contains larger aggregates such as gravel or crushed rocks. These aggregates are normally in the bulk but not on the surface. One can therefore assume that the adsorption on both concrete and mortar is defined by the same cementitious matrix. From this perspective, cement mortar can be considered a surrogate for concrete, for surface adsorption study purposes. Intact mortar coupons were used directly in the tests as opposed to crushed or pulverised samples. The adsorption values were attributed to the exposed surface area of a coupon instead of the mass of a crushed sample. This was done based on practical considerations: it would be easier for first responders to measure the surface area of a contaminated building, rather than its mass.

2. Experimental

2.1. Test coupons

Anhydrous cesium chloride (CsCl) 99.99% was purchased from Sigma–Aldrich. Cement mortar coupons were fabricated in-house, using Portland cement, sand and deionized water in a 1:5:5 mass ratio. The coupons were cast in $5.0 \text{ cm} \times 5.0 \text{ cm} \times 1.5 \text{ cm}$ rectangular molds. The average dimensions of the coupons were therefore approximately $5.0 \text{ cm} \times 5.0 \text{ cm} \times 1.5 \text{ cm}$ with the total external surface area of about 80 cm^2 . The coupons were stored prior to experiments at an ambient temperature for approximately 60 days for the mortar to cure.

Each test coupon had the shape of a rectangular prism. Its volume was proportional to the cube of the linear dimension while the surface area was proportional to the square. The surface area was therefore proportional to the volume to the power of $2/3$. In this study, the coupons were weighted and an average weight m_{av} was calculated. This weight corresponded to the average surface area S_{av} of 80 cm^2 . The surface area of a particular coupon S was then estimated based on its mass m : $S = S_{av}(m/m_{av})^{2/3}$ and was found to be in the range of $76.1\text{--}84.1 \text{ cm}^2$ as shown in Table 1. It was easier to measure the mass instead of dimension and take into account surface imperfections.

2.2. Adsorption experiments

As listed in Table 1, a series of experiments were carried out using several different initial cesium concentrations C_0 ranging from 0.0103 to 10.88 mg L^{-1} . Each cement mortar coupon was completely immersed into the cesium solution and secured by plastic clamps. All tests were performed using the Fisher brand polypropylene beakers with 1000 mL of initial solutions. The solutions were thoroughly mixed during the experiment at the constant speed of 600 rpm using magnetic stirrers. The tests were performed in a temperature-controlled environment at 278 , 286 , 294 and 313 K . Samples were taken at the following time elapsed from the beginning of the tests: 0 , 0.5 , 2 , 3 , 4 , 5 and 6 h . After the first day, sampling was done once a day except weekends, until no significant change in cesium concentration was observed. It was assumed that adsorption equilibrium was attained at this point. Each sample had a volume of 10 mL . The samples were stored in polystyrene test tubes.

The mass of adsorbed cesium (μg) was determined from a mass balance, as a difference between the initial mass of cesium in solution and that remaining at a time of sampling. The change in overall volume of the solution with every 10 mL sample was taken into account in this mass balance. After each sampling, the remaining solution volume and the mass of cesium in it were recalculated to account for losses. The cesium surface concentration ($\mu\text{g cm}^{-2}$) was calculated by dividing the mass of adsorbed cesium on cement mortar by the surface area of a coupon.

2.3. ICP-MS analysis

The aqueous solutions of cesium were analyzed via a Thermo X Series II inductively coupled plasma mass spectrophotometry (ICP-MS) in a fully quantitative analytical method in standard mode. An internal standard of 0.1 mg L^{-1} rhodium in 4% hydrochloric acid was used to monitor the analysis. The instrument was calibrated by 0.1 and 1 mg L^{-1} standard cesium solutions before running samples and checked by the same solutions after running samples. All experimental data were the average of three to five replications.

Table 1
Summary of test conditions and results for adsorption of cesium on cement mortar.

Sample	T (K)	m (g)	S (cm ²)	C ₀ (mg L ⁻¹)	C _e (mg L ⁻¹)	q _e (μg cm ⁻²)
A	294	70.14	79.20	0.0103	0.0069	0.0395
B	294	66.10	76.13	0.0452	0.0317	0.1664
C	294	73.00	81.34	0.2126	0.1728	0.4745
D	294	70.25	79.29	1.019	0.889	1.557
E	294	74.39	82.37	10.88	8.837	22.34
F	286	72.59	81.04	0.0653	0.0224	0.4883
G	286	72.50	80.97	0.2972	0.1116	2.090
H	286	73.83	81.96	1.038	0.6432	4.952
I	286	76.70	84.07	10.05	7.151	31.34
J	278	67.25	77.01	1.041	0.7819	2.255
L	313	71.56	80.27	1.010	0.951	0.6671

T = temperature; m = mass of the coupon; S = surface area of the coupon; C₀ = initial concentration of cesium in solution; C_e = equilibrium concentration of cesium in solution; q_e = equilibrium concentration of cesium on coupon surface.

2.4. Quality assurance and control

Cesium is known to strongly adsorb on glassware. To eliminate the adsorption on glass, polypropylene test beakers, polystyrene test vials, and polyethylene-coated clams were used in the tests.

Mortar coupons were visually examined after fabrication and those containing cracks and crevices were eliminated from tests. Coupons whose weight differed from an average weight by more than 10% were also eliminated. This was done to limit the effect of coupon imperfection on adsorption characteristics.

A control and a blank test, as well as duplicates of each set of initial cesium concentration were performed. In the control test, a beaker was filled with cesium solution and concentrations were monitored over time; however, no cement mortar coupon was immersed. The control experiments revealed no change in cesium concentration over time. This indicated neither interaction with the test beaker nor a loss of solution volume due to evaporation.

A blank sample contained just deionized water and a cement mortar coupon immersed into it. The blank test was used to verify the possible desorption (leaching) of cesium, which might be naturally present in cement mortar, into the deionized water. The result of the blank experiment revealed that cesium concentration released from cement mortar at room temperature after 12 days of adsorption tests, was 1.51 μg L⁻¹. This concentration was found to be negligible in comparison to the cesium concentrations at equilibrium for all the tests carried out. The release of naturally occurring cesium from test coupons was therefore considered to be too low to interfere with adsorption results. Experiments for different initial cesium concentrations were duplicated and the results revealed a good reproducibility, within 5–9% experimental error. The details of test conditions are provided in Table 1.

3. Results and discussion

3.1. Kinetic experiments

The cesium surface concentration as a function of time at room temperature (294 K) is shown in Fig. 1. As expected, the adsorption process initially went rapidly and then continued at a slower rate until equilibrium was achieved. The mass of adsorbed cesium at equilibrium depended on the initial cesium concentration. The rates of adsorption dq/dt in the first 4 h at room temperature for the initial concentrations of 0.0452, 1.019, and 10.88 mg L⁻¹ at 294 K are shown in Fig. 2. The rate of adsorption was orders of magnitude greater for the higher initial concentration compared to that for the lower concentrations. This was due to higher driving force of adsorption at higher initial concentrations. Adsorption equilibrium for all initial concentrations appeared to be attained within approximately 12 days (288 h). It was assumed that a relatively long time required to reach the equilibrium was caused by slow pore diffu-

sion due to narrow pores of the cement mortar. Like most natural or synthetic minerals, cement mortar has wide pore size distribution. Kumar and Bhattacharjee [18] reported the porosity of concrete samples varying from 9.26% to 33.7%. Pore diameters ranged from less than 10.6 nm to greater than 106 nm; however, in most cases fewer than 6% of the pores had diameter larger than 106 nm. During the adsorption experiments, larger pores were filling with cesium relatively rapidly while smaller ones were filling slowly. For the smaller pores, diffusion was likely the determining step in the mass transfer. Similar trends were reported [19,20] for kinetics of cesium adsorption on granite.

Kinetics of adsorption of cesium on cement mortar was studied at 294 K by using first order reaction model [20–22], the pseudo-second order reaction model [23–26] and the isothermal intra-particle diffusion model [27,28].

The first order and the pseudo-second order adsorption kinetics are described by Eqs. (1) and (2), respectively.

$$\frac{dq_t}{dt} = k_1 (q_e - q_t) \quad (1)$$

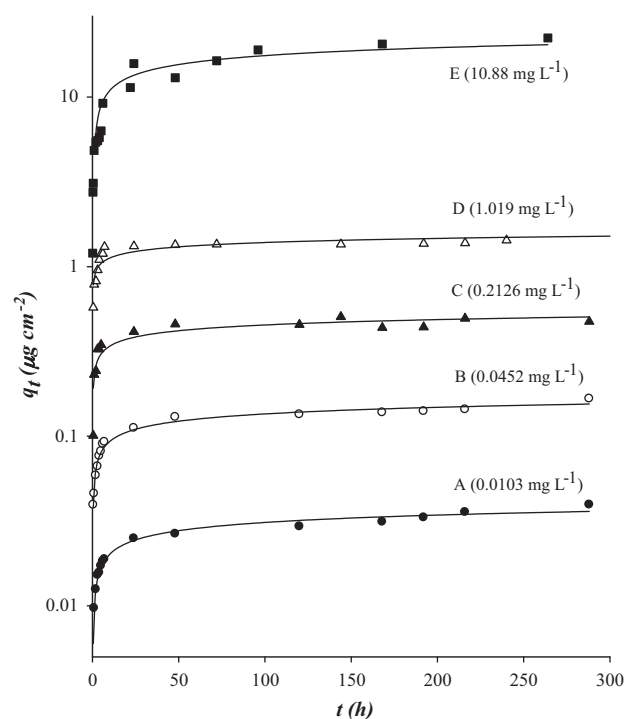


Fig. 1. Change of cesium surface concentration q_t at 294 K as a function of time for several initial concentrations of cesium in solution.

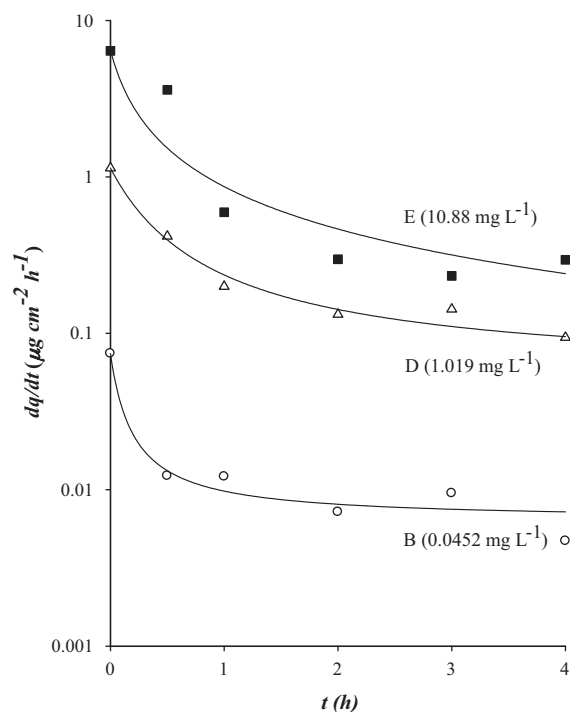


Fig. 2. Rate of adsorption of cesium on cement mortar, dq/dt , as a function of time at 294 K for several initial concentrations of cesium in solution up to 4 h of testing.

$$\frac{dq_t}{dt} = k_2(q_e - q_t)^2 \quad (2)$$

where t is time (h); q_t and q_e are cesium surface concentrations ($\mu\text{g cm}^{-2}$) on coupon at time t and at equilibrium, respectively. k_1 and k_2 are the first order and pseudo-second order reaction constants (h^{-1} and $\text{cm}^2 \mu\text{g}^{-1} \text{h}^{-1}$), respectively.

By integrating Eqs. (1) and (2) over time t and knowing that the initial surface concentration is zero, the following equations can be produced for the first order

$$\ln(q_e - q_t) = \ln q_e - k_1 t \quad (3)$$

and the pseudo-second order models:

$$\frac{t}{q_t} = \frac{1}{q_e} t + \frac{1}{k_2 q_e^2} \quad (4)$$

Eqs. (3) and (4) can be plotted as $\ln(q_e - q_t)$ vs. t and t/q_t vs. t , respectively. A linear dependency would mean a good fit between experimental results and the model.

The intra-particle diffusion model is described as follows:

$$q_t = k_p t^{1/2} \quad (5)$$

Eq. (5) can be linearized with respect to time t .

$$\ln q_t = \ln k_p + \frac{1}{2} \ln t \quad (6)$$

Similarly to the first order and the pseudo-second order models, a linear dependency of $\ln q_t$ vs. $\ln t$ would mean a good fit between the model and the test results.

Fig. 3 presents kinetic data fit at 294 K according to the three models considered. One can see that only the pseudo-second order kinetic model has a good linear fit throughout the entire test duration, although the other models showed linearity in early stages of the tests. The pseudo-second order model can therefore be chosen to describe the kinetics for adsorption of cesium by cement mortar and possibly, by other cementitious matrices like concrete. Similar interpretation of the test results was attempted by Bouzidi

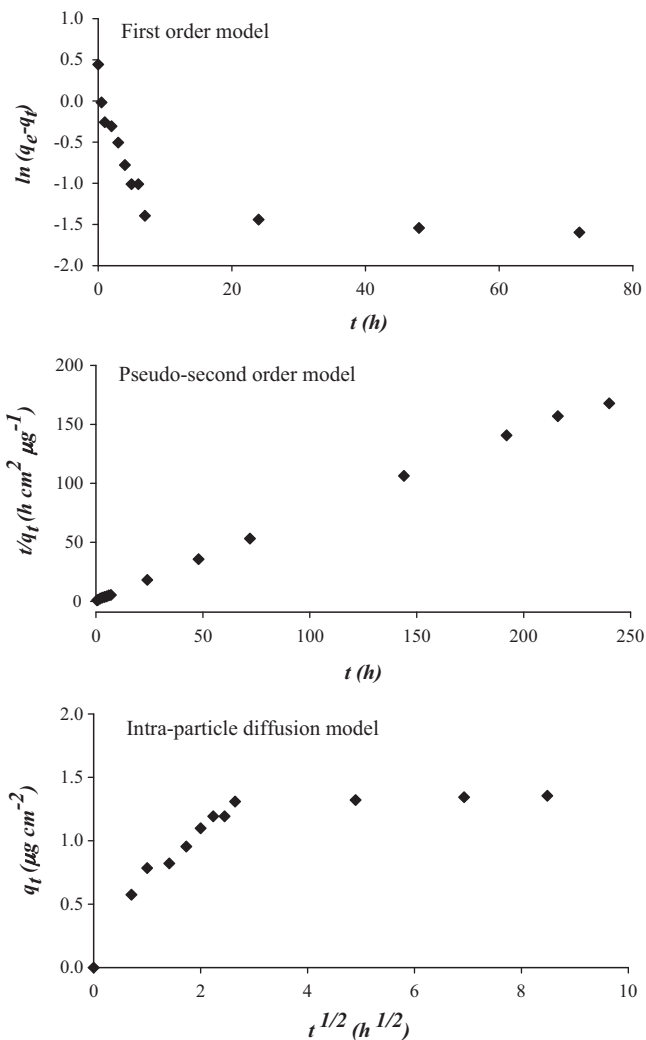


Fig. 3. Comparison of first order, pseudo-second order, and intra-particle diffusion kinetic data fits at 294 K for initial cesium concentration of 1.019 mg L^{-1} in solution.

et al. [29] and Sheha and Metwally [30]. They reported that the adsorption of cesium on soil and magnetite was better described by the pseudo-second order kinetic model compared to the first order kinetic model. Wang et al. [31] and Tsai et al. [20] used the first order model to describe the adsorption of cesium on minerals such as laterite and granite. They did not use the pseudo-second order model so it is unknown whether the former indeed produced a better fit. On the other hand, Karamains and Assimakopoulos [32] who used both models to interpret the adsorption of cesium on aluminum-pillared montmorillonite, reported that the first order model produced a better fit. This difference in modeling results suggests that the kinetics of the adsorption process is affected by the chemical composition and porosity of the adsorbent. It is likely that differences in test conditions also play a role.

The pseudo-second order fit for temperatures 278, 286, 294, and 313 K is shown in Fig. 4. The linearity of t/q_t vs. t function remains good for all the temperatures studied. According to Eq. (4), the slope is equivalent to $1/q_e$ where q_e is the equilibrium surface concentration. The intercept in the t/q_t vs. t dependency is equal to $k_2^{-1} q_e^{-2}$ and can therefore be used to calculate the pseudo second order rate constant, k_2 . The k_2 values at different temperatures for adsorption of approximately 1.0 mg L^{-1} initial cesium solution on cement mortar are listed in Table 2. The rate constant of adsorption increased as the temperature increased. This was due to the fact that a higher temperature resulted in a faster diffusion of cesium ions towards

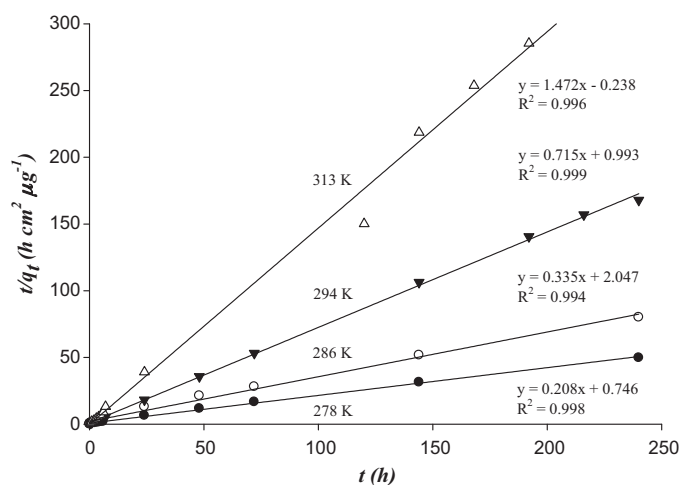


Fig. 4. Pseudo-second order kinetic data fit at different temperatures, C_0 approximately 1.0 mg L^{-1} .

the surface of cement mortar and inside the pores of the cement mortar coupons.

The rate of adsorption depends on the activation energy of adsorption E_a and the temperature. Its dependency can be interpreted by the Arrhenius equation [33].

$$k_2 = Ae^{-E_a/RT} \quad (7)$$

Eq. (7) can be presented in a logarithmic form:

$$\ln k_2 = \ln A - (E_a/RT) \quad (8)$$

where A is an Arrhenius constant that is independent of temperature, E_a is the activation energy (J mol^{-1}), T is the temperature (K) and R is the universal gas constant, $8.314 \text{ J K}^{-1} \text{ mol}^{-1}$. The plot of $\ln k_2$ vs. $1/T$ is a straight line with the slope equal to $-E_a/R$ which allows the calculation of the activation energy. This plot is shown in Fig. 5. The pseudo-second rate constant k_2 is used since the pseudo-second order kinetic model best describes the adsorption of cesium on cement mortar. The activation energy of adsorption is known to be an indicator of a type of bond between the adsorbent and the adsorbate: E_a lower than 20 kJ mol^{-1} of adsorbate usually suggests physical adsorption and associated weaker bonds. The value of E_a which is higher than 40 kJ mol^{-1} indicates stronger bonds and chemical adsorption, or chemisorption [34]. For the adsorption of cesium in the range from 278 to 313 K, E_a was calculated from the slope of Fig. 5 and determined to be 55.9 kJ mol^{-1} . This value is in line with that reported for adsorption of cesium on laterite [34] and clinoptilolite minerals [35]. The value of E_a which is greater than the threshold of 40 kJ mol^{-1} suggests that the interaction between cesium ions and cement mortar is dominated by chemisorption rather than physical adsorption.

3.2. Equilibrium experiments

The equilibrium concentrations in solution C_e and on the surface q_e were determined for each initial concentration C_0 and summa-

Table 2
Calculated k_2 values for adsorption of 1.0 mg L^{-1} initial cesium solution on cement mortar at different temperatures.

Sample	T (K)	k_2 ($\text{cm}^2 \mu\text{g}^{-1} \text{ h}^{-1}$)
J	278	0.027
H	286	0.048
D	294	0.115
L	313	0.387

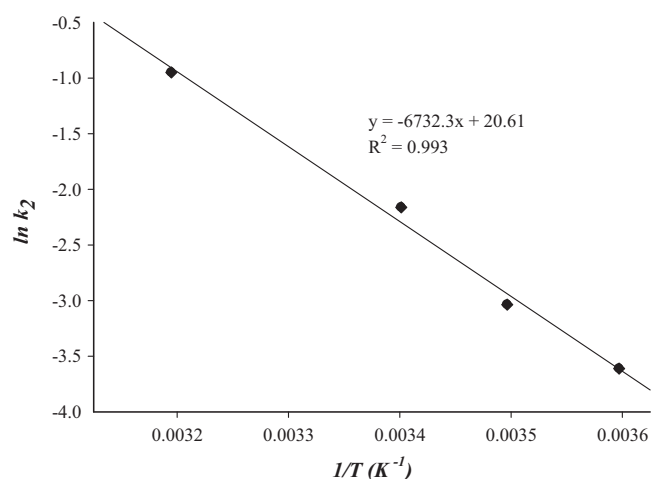


Fig. 5. Arrhenius plot of $\ln k_2$ vs. $1/T$ for approximately 1.0 mg L^{-1} initial cesium concentration.

rized in Table 1. Overall between 5 and 59% of cesium was adsorbed on cement mortar at equilibrium. The quantities of adsorbed Cs at equilibrium ranged from 0.0395 to $22.34 \mu\text{g cesium/cm}^2$ of coupon surface. At the same time, the equilibrium concentration in solution ranged from 0.0069 mg L^{-1} to 8.837 mg L^{-1} .

As shown in Table 1, for most tests with the same initial concentration of approximately 1.0 mg L^{-1} , a higher temperature corresponded to a lower equilibrium surface concentration, q_e . This observation suggests that adsorption of cesium by cement mortar is an exothermic process. Slightly lower q_e for 278 K (5°C) possibly due to changes in characteristics of cement mortar-water systems at temperatures close to freezing.

The relationship between the amount of adsorbed cesium and its concentration in the solution at equilibrium is described by an adsorption isotherm. For liquid systems, the relationship between C_e and q_e can be defined by either Langmuir model [35] or by Freundlich model [36]. The models are described by Eq. (9) (Langmuir) and Eq. (10) (Freundlich):

$$q_e = \frac{q_m b C_e}{1 + b C_e} \quad (9)$$

$$q_e = K_F C_e^{1/n} \quad (10)$$

where b is the Langmuir constant and q_m is the maximum saturation capacity at the isotherm temperature; K_F is the Freundlich constant and n is greater than 1.

The above equations can be rearranged into linear format as Eqs. (11) and (12), respectively.

$$\frac{1}{q_e} = \frac{1}{q_m} + \left(\frac{1}{b q_m} \right) \left(\frac{1}{C_e} \right) \quad (11)$$

$$\log q_e = \log K_F + \frac{1}{n} \log C_e \quad (12)$$

Linear dependencies of $1/q_e$ vs. $1/C_e$ or $\log q_e$ vs. $\log C_e$ would then suggest a good fit with either the Langmuir or the Freundlich model.

The equilibrium data obtained for adsorption of cesium by cement mortar coupons at 286 K and 294 K are shown in Fig. 6. The solid trendlines representing the Freundlich model fit the experimental data well. Freundlich isotherm is therefore the model which covers all considered equilibrium concentrations in this study. In the lower equilibrium concentration range, however, both Langmuir and Freundlich models are well fitted to the experimental data. Freundlich constant K_F at 286 K and 294 K was calculated to

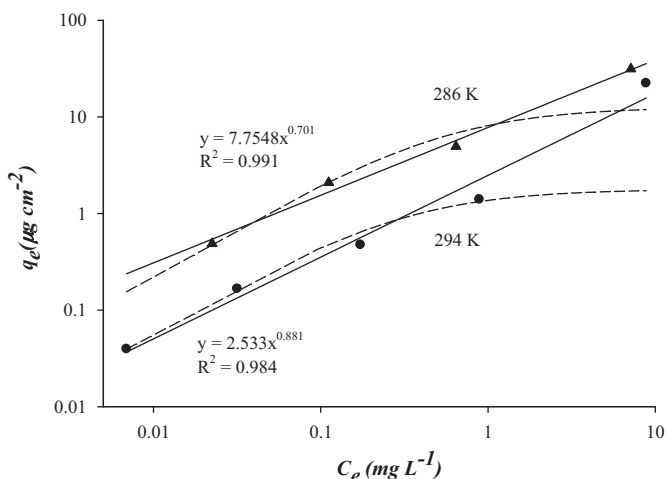


Fig. 6. Freundlich (solid lines) and Langmuir (dashed lines) isotherms at 286 and 294 K in logarithmic scale. The points represent the experimental data and the curves shows the corresponding isotherms.

be $7.754 \mu\text{g}^{0.30} \text{mL}^{0.70} \text{cm}^{-2}$ and $2.483 \mu\text{g}^{0.15} \text{mL}^{0.85} \text{cm}^{-2}$, respectively. Dimensionless Freundlich parameter n was calculated to be 1.429 and 1.182, respectively.

Based on adsorption equilibrium model theories, whenever the Langmuir isotherm dominates, it implies on the concept of a monolayer adsorption. On the other hand, if Freundlich isotherm prevails, it entails that possibly a multi-layer adsorption is involved. Our results show that in the overall range of concentrations, Freundlich isotherm fits better than the Langmuir isotherm. At low concentrations though, Langmuir isotherm also produces a satisfactory fit. This likely suggests that a monolayer adsorption prevails in a lower concentration range followed by a multi-layer adsorption at higher concentrations. It should be noted that the multi-layer adsorption may also happen inside the pores, in addition to coupon surface.

4. Conclusions

The adsorption of cesium from aqueous solutions on cement mortar was investigated in the range of initial cesium concentrations of $0.0103\text{--}10.88 \text{ mg L}^{-1}$ and in the range of temperatures of $278\text{--}313 \text{ K}$. It took approximately 12 days to reach adsorption equilibrium. The quantities of adsorbed Cs at equilibrium ranged from 0.0395 to $22.34 \mu\text{g cesium/cm}^2$ of coupon surface. At the same time, the equilibrium concentration in solution ranged from 0.0069 mg L^{-1} to 8.837 mg L^{-1} .

The pseudo-second order kinetic model produced a good fit with the experimental kinetic data. The adsorption rate constant increased with an increase in temperature, likely resulting from a faster diffusion. The activation energy of adsorption determined from the Arrhenius equation was found to be equal to 55.9 kJ mol^{-1} . It suggests that the interaction between cesium ions and cement mortar is dominated by chemical adsorption.

The relationship between concentration of the adsorbed cesium q_e and that of cesium remaining in the solution at equilibrium C_e was better described by Freundlich model rather than by Langmuir model, for both temperatures studied. This indicates the prevalence of a multi-layer adsorption of cesium on cement mortar, at high initial cesium concentrations in test solutions. The surface concentration of adsorbed cesium at equilibrium decreased as temperature increased, suggesting that adsorption was an exothermic process.

Acknowledgements

Funding for this research was provided by the Chemical, Biological, Radiological, Nuclear, and Explosive Research and Technology Initiative (CRTI) under project 06-0156RD. The authors thank Pervez Azmi (Environment Canada), Emily Snyder and Sangdon Lee (US Environmental Protection Agency), and Marc Desrosiers (DRDC Canada) for their valuable contributions.

References

- [1] R. Chard, D. Maxwell-Downing, S. Mitchell, B. Burlingame, M. Ogg, J. Blanchard, The best of clinical issues, *AORN J.* 90 (6) (2009) S63–S77.
- [2] A. Lykknes, Radiation everywhere!, *Endeavour* 29 (4) (2005) 136.
- [3] M.I. Balonov, L.R. Anspaugh, A. Bouville, I.A. Likhtharev, Contribution of internal exposures to the radiological consequences of the Chernobyl accident, *Radiat. Prot. Dosim.* 127 (1–4) (2007) 491–496.
- [4] E. Korobova, V. Linnik, N. Chizhikova, The history of the Chernobyl 137Cs contamination of the flood plain soils and its relation to physical and chemical properties of the soil horizons (a case study), *J. Geochem. Explor.* 96 (2–3) (2008) 236–255.
- [5] F. Steinhauser, Chernobyl and Goiânia lessons for responding to radiological terrorism, *Health Phys.* 89 (5) (2005) 566–574.
- [6] IAEA (International Atomic Energy Agency) Reducing Risks in the Scrap Metal Industry: Sealed Radioactive Sources. Report IAEA/PI/A.83/05-09511. Vienna, Austria, 2005.
- [7] M.Y. Miah, K. Volchek, W. Kuang, H. Tezel, Kinetic and equilibrium studies of cesium adsorption on ceiling tiles from aqueous solutions, *J. Hazard. Mater.* 183 (1–3) (2010) 712–717.
- [8] G. Kosakowski, S.V. Churakov, T. Thoelen, Diffusion of Na and Cs in montmorillonite, *Clay Clay Miner.* 56 (2) (2008) 190–206.
- [9] T. Wang, M. Li, W. Yeh, Y. Wei, S. Teng, Removal of cesium ions from aqueous solution by adsorption onto local Taiwan laterite, *J. Hazard. Mater.* 160 (2–3) (2008) 638–642.
- [10] S. Staunton, C. Dumat, A. Zsolnay, Possible role of organic matter in radio caesium adsorption in soils, *J. Environ. Radioact.* 62 (2002) 1–15.
- [11] E.K. Duursama, D. Eisma, Theoretical, experimental and field studies concerning reactions of radioisotopes with sediment and suspended particles of the Sea: Part C: applications to field studies, *Neth. J. Sea Res.* 6 (1973) 265–324.
- [12] S. Komareni, D.M. Roy, Tobermorites: a new family of cation exchangers, *Science* 221 (4611) (1981) 647–648.
- [13] Y. Asakuma, S. Takeda, K. Maeda, K. Fukui, Kinetic and theoretical studies of metal ion adsorption in KDP solution, *Appl. Surf. Sci.* 225 (2009) 4140–4144.
- [14] O.P. Shrivastava, R. Shrivastava, Cation exchange applications of synthetic tobermorite for the immobilization and solidification of cesium and strontium in cement matrix, *Bull. Mater. Sci.* 23 (2000) 515–520.
- [15] J.F. Real, F. Persin, C. Claret, Mechanisms of desorption of ^{134}Cs and ^{85}Sr aerosols deposited on surfaces, *J. Environ. Radioact.* 62 (2002) 1–15.
- [16] O.P. Shrivastava, V. Taruna, P.K. Wattal, Intrinsic sorption potential of aluminum-substituted calcium silicate hydroxyl hydrate for $^{137}\text{Cesium}$, *Adv. Cem. Bas. Mater.* 2 (1995) 80–83.
- [17] S.L. Marusin, Ancient cement mortar structures, *Cem. Mortar Int.* 18 (1996) 56–58.
- [18] R. Kumar, B. Bhattacharjee, Porosity, pore size distribution and in situ strength of concrete, *Cem. Concr. Res.* 33 (2003) 155–164.
- [19] S. Tsai, T. Wang, W. Wei, W. Yeh, Y. Jan, S. Teng, Kinetics of Cs adsorption/desorption on granite by a pseudo first order reaction model, *J. Radioanal. Nucl. Chem.* 275 (3) (2008) 555–562.
- [20] S. Tsai, T. Wang, M. Li, Y. Wei, S. Teng, Cesium adsorption and distribution onto crushed granite under different physicochemical conditions, *J. Hazard. Mater.* 161 (2009) 854–861.
- [21] A.K. Bhattacharya, C. Vekobachar, Removal of cadmium (II) by low cost adsorbents, *J. Environ. Eng.* 110 (1) (1984) 110–122.
- [22] N. Roostai, F.H. Tezel, Removal of phenol from aqueous solutions by adsorption, *J. Environ. Manage.* 70 (2004) 157–164.
- [23] N. Chiron, R. Guilet, E. Deydier, Adsorption of Cu(II) and Pb(II) onto a grafted silica: isotherms and kinetic models, *Water Res.* 37 (2003) 3079–3086.
- [24] Y.S. Ho, A.E. Ofomaja, Kinetic studies of copper ion adsorption on palm kernel fiber, *J. Hazard. Mater.* B137 (2006) 1796–1802.
- [25] I. Nouri, I. Ghoubbane, O. Hamadaoui, M. Chiba, Batch sorption dynamics and equilibrium for the removal of cadmium ions from aqueous phase using wheat barn, *J. Hazard. Mater.* 149 (2007) 115–125.
- [26] N. Bektas, B. Akman, S. Kara, Kinetic and equilibrium studies in removing lead ions from aqueous solutions by natural sepiolite, *J. Hazard. Mater.* B112 (2004) 115–122.
- [27] D.M. Ruthven, Principles of Adsorption and Adsorption Processes, Wiley-Interscience Press, New York, 1984.
- [28] G. McKay, The adsorption of dyestuffs from aqueous solutions using activated carbon: analytical solution based on batch adsorption based on external mass transfer and pore diffusion, *J. Biochem. Eng.* 27 (1983) 187–194.
- [29] A. Bouzidi, F. Souahi, S. Hanini, Sorption behavior of cesium on Aim Oussera soil under different physicochemical conditions, *J. Hazard. Mater.* 184 (2010) 640–646.

- [30] R.R. Sheha, E. Metwally, Equilibrium isotherm modeling of cesium adsorption onto magnetic materials, *J. Hazard. Mater.* 143 (2007) 354–361.
- [31] T.H. Wang, M.H. Li, W.C. Yeh, Y.Y. Wei, S.P. Teng, Removal of cesium ions from aqueous solution by adsorption onto local Taiwan laterite, *J. Hazard. Mater.* 160 (2008) 638–642.
- [32] D. Karamanis, P.A. Assimakopoulos, Efficiency of aluminum-pillared montmorillonite on the removal of cesium and copper from aqueous solutions, *Water Res.* 41 (2007) 1897–1906.
- [33] S. Arrhenius, Über die Reaktionsgeschwindigkeit bei der Inversion von Rohrzucker durch Säuren, *Zeitschrift für Physikalische Chemie* 4 (1889) 226–248.
- [34] T. Shahwan, D. Akar, A.E. Eroğlu, Physicochemical characterization of the retardation of aqueous Cs⁺ ions by natural kaolinite and clinoptilolite minerals, *J. Colloid Interface Sci.* 285 (2005) 9–17.
- [35] I. Langmuir, The adsorption of gases on plane surfaces of glass, mica and platinum, *J. Am. Chem. Soc.* 40 (1918) 1361–1403.
- [36] H. Freundlich, *Kapillarchemie*, Akademische Bibliothek, Leipzig, 1909.